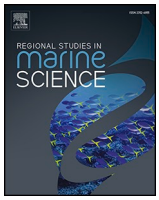
Regional Studies in Marine Science 102 (2026) 105474



Contents lists available at ScienceDirect

Regional Studies in Marine Science

journal homepage: www.elsevier.com/locate/rsma





Geochemical reference functions as a tool for detecting environmental change: Application to trace-elements in the Sacca di Goro (Italy)

Antonello Aquilano [*,1], Joana Buoninsegni [2], Elena Marrocchino [*,3], Carmela Vaccaro [4]

University of Ferrara, Department of Environmental and Prevention Sciences, Ferrara, Italy

ARTICLE INFO

Keywords:
Sediment geochemistry
Po Delta
Transitional environments
Environmental change

ABSTRACT

Assessing trace-element distributions in lagoon sediments requires accounting for sedimentological and lithogenic controls that influence their content. Conventional sediment assessment indices provide standardized measures of enrichment and contamination, but rely on fixed reference values that may not fully capture the geochemical characteristics of a specific system. A pristine or pre-industrial reference would provide a direct basis for defining natural background conditions, but such material can be difficult to identify in highly dynamic environments such as lagoon, and no specific reference is available for the Sacca di Goro (Po Delta, Italy). A sediment dataset collected during previous monitoring of the lagoon in 2003–2005 was used to characterize the geochemical structure of the system and establish Historical Geochemical Reference Functions (HGRFs). These functions were applied to sediments collected in 2023 to identify departures from the reference relationships. HGRFs identified no significant departures for Pb, Cu and V, whereas Ni and Cr showed positive departures. Zn also showed a positive pattern, although this was not statistically significant after accounting for spatial dependence and multiple comparisons. These results indicated that the recent behaviour of Ni and Cr differs from the relationships represented by the 2003–2005 dataset. The HGRFs results were also considered alongside conventional sediment assessment indices, providing an additional perspective on the geochemical differences between the two datasets. HGRFs provide a complementary, system-specific reference based on empirical geochemical relationships rather than fixed regional values. Their application allows recent observations to be evaluated against the geochemical structure documented by previous monitoring and helps identify element-specific departures that may warrant further investigation.

1. Introduction

Transitional waters represent complex, heterogeneous and dynamic systems whose response to nutrient and organic matter inputs from terrestrial catchments depends on local geomorphological and hydrological conditions, as well as to global environmental changes (Crossland et al., 2005; Newton et al., 2014).

Anthropogenic pressures constitute a major source of stress for these ecosystems, particularly as a consequence of increasing urbanization and economic development in surrounding areas (Newton et al., 2014). The intensification of human activities (e.g. navigation, agriculture, river regulation) can significantly alter both landscape morphology and ecosystem functioning. Urban pollution represents one of the main threats to coastal ecosystems, contributing to increased biological productivity, eutrophication, biodiversity loss and impacts on fisheries (Amir et al., 2019; Gao et al., 2012; Rahhou et al., 2022).

The pressures affecting these environments have attracted increasing scientific and political attention, leading European institutions to develop specific regulatory frameworks for their protection. In this context, the Marine Strategy Framework Directive (MSFD) was adopted in 2008 and currently represents the main legislative framework of the European Union for the protection and sustainable management of the marine environment (The European Parliament, 2008).

The Sacca di Goro (Fig. 1) is a shallow coastal lagoon located in the

* Corresponding authors.
E-mail addresses: qlnnnl@unife.it (A. Aquilano), mrrlne@unife.it (E. Marrocchino).
[1] https://orcid.org/0000-0002-3291-1445
[2] https://orcid.org/0009-0004-8276-8247
[3] https://orcid.org/0000-0001-7320-0327
[4] https://orcid.org/0000-0002-4954-8697

https://doi.org/10.1016/j.rsma.2026.105474
Received 14 July 2026; Received in revised form 31 August 2026; Accepted 16 September 2026
Available online 23 September 2026
2352-4855/© 2026 The Author(s). Published by Elsevier B.V. This is an open access article under the CC BY license (http://creativecommons.org/licenses/by/4.0/).

southern sector of the Po River Delta (northern Adriatic Sea, Italy), covering approximately 35 km^2 (Maicu et al., 2021). The lagoon represents a transitional environment, whose hydrological and sedimentological dynamics are strongly influenced by freshwater and sediment inputs from the Po River system (Simeoni et al., 2007; Viaroli et al., 2007).

The lagoon receives freshwater from the Po di Volano, Canal Bianco, Po di Goro and Po della Donzella (Fig. 1). These watercourses act as major pathways for the transport of nutrients and fine-grained sediments derived from the Po catchment, exerting a strong influence on sediment composition and geochemical characteristics within the lagoon (Zaldívar et al., 2003; Marinov et al., 2008). Water circulation and sediment deposition are further controlled by the presence of a barrier spit separating the lagoon from the Adriatic Sea (Scanno di Goro), which regulates water exchange and promotes the accumulation of fine sediments within the basin (Simeoni et al., 2007).

Beyond its ecological significance, the Sacca di Goro represents one of the most important aquaculture areas in the northern Adriatic and has historically supported extensive production of the Manila clam (*Ruditapes philippinarum*) (Marinov et al., 2008).

The lagoon has also an important role in supporting ecosystem services and contributing to carbon sequestration through biocalcification processes (Tamburini et al., 2022). Given the ecological and socio-economic relevance of the lagoon, assessing the current sediment quality and geochemistry in relation to historical conditions is of particular importance for the sustainable management of this transitional environment.

Several approaches have been proposed for the assessment of trace-elements contamination in sediments, including for example: enrichment factors (EF), geoaccumulation indices (Igeo), contamination factors (CF), pollution load indices (PLI), regional background values and sediment-quality guidelines, etc. (Dung et al., 2013). These methods provide valuable information on contamination status, relative enrichment and potential ecological significance and are widely applied in sediment-quality assessments. Their interpretation can be complemented by considering sediment texture and other physicochemical characteristics, which may influence trace-element distributions in estuarine sediments (Jose et al., 2026). In particular, sediment grain size can affect trace-element retention and contribute to spatial variability in sediment metal concentrations (Dev et al., 2026). However, these indices are generally based on comparisons with fixed reference values and may not explicitly account for the influence of grain size, mineralogical composition, sediment provenance and other natural controls on trace-element distributions. Previous studies have highlighted that such factors can exert a primary influence on element contents, complicating the distinction between natural variability and anthropogenic enrichment (Bábek et al., 2015; Matys Grygar and Popelka, 2016).

In the context of the Sacca di Goro, regional geochemical reference values have been proposed by Migani et al. (2015). These values provide a useful regional benchmark for conventional sediment assessment, but they were not specifically established for the Sacca di Goro and as fixed reference values, they do not describe the geochemical relationships between trace elements and the sedimentological and lithogenic factors characterizing this environment. A pristine or pre-industrial sediment

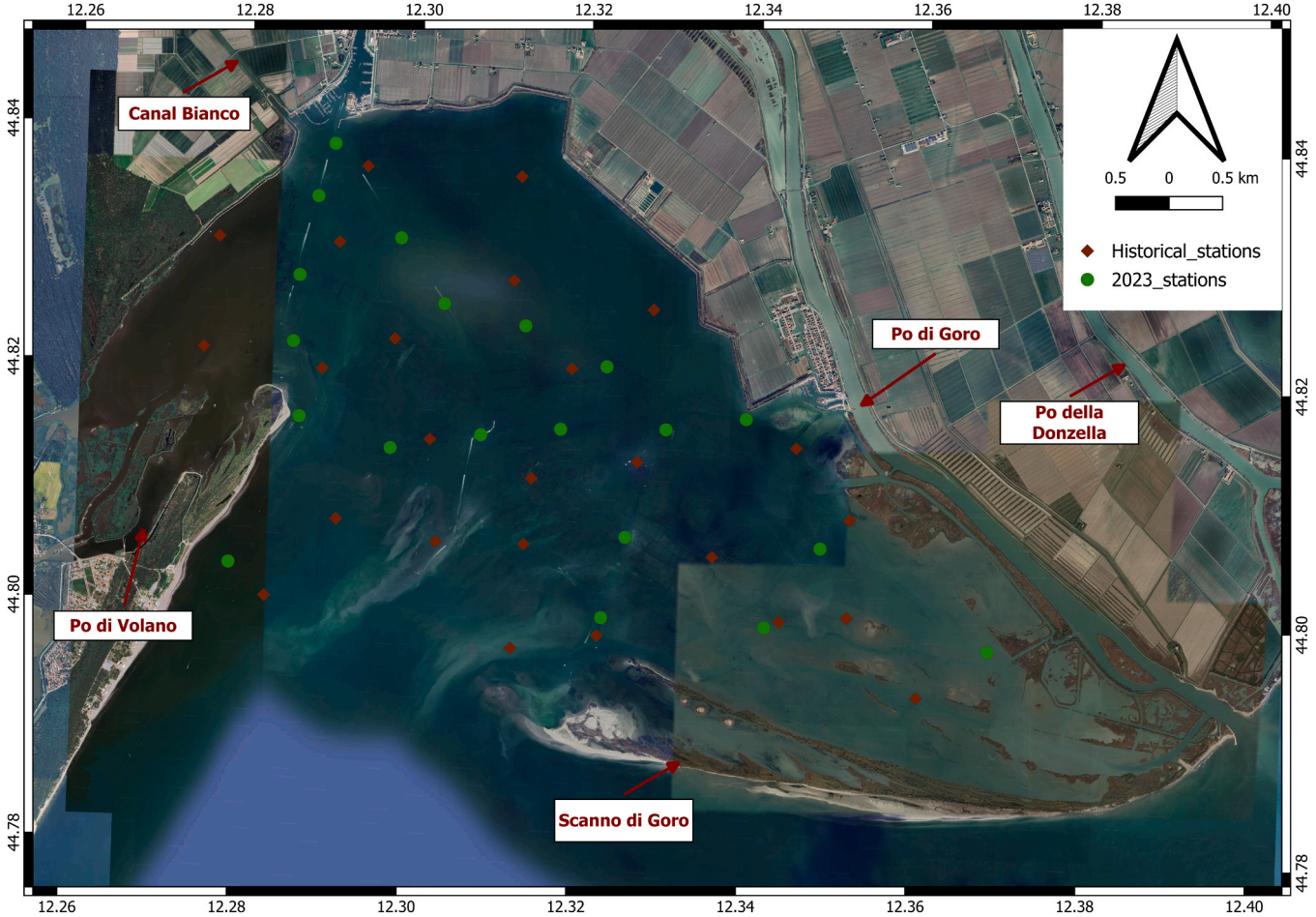


Fig. 1. Satellite image of the Sacca di Goro. The map shows the main watercourses supplying sediments to the Sacca di Goro (Canal Bianco, Po di Volano, Po di Goro, and Po della Donzella), as well as the sandy barrier separating and protecting the lagoon from the Adriatic Sea (Scanno di Goro). Historical sampling stations are indicated by red diamonds, whereas the sampling stations surveyed in December 2023 as part of this study are indicated by green circles.

record would provide a more direct basis for defining natural background conditions. However, such reference material is often difficult to obtain reliably in coastal and lagoonal environments, where long histories of sediment accumulation, reworking and anthropogenic influence may make it difficult to identify sediments that truly represent undisturbed conditions. No pristine or pre-industrial sediment dataset is currently available for the Sacca di Goro. The historical monitoring record nevertheless contains information that cannot be captured by a single reference value, as it documents the relationships between trace elements and the sedimentological and geochemical characteristics of the lagoon during a defined historical period. The present study aims to formalize these empirical relationships as Historical Geochemical Reference Functions (HGRFs), and to investigate their potential to provide a system-specific reference for evaluating recent sediment observations. Unlike conventional indices, which assess elemental content relative to fixed reference values, the HGRF approach is designed to evaluate recent observations in relation to the geochemical relationships represented by an historical dataset.

The objectives of this study are therefore to: (i) characterize the sedimentological and geochemical relationships underlying trace-element distributions in the Sacca di Goro and identify suitable lithogenic proxies; (ii) develop HGRFs based on the historical sediment dataset; (iii) apply the HGRFs to recent sediments to identify departures from the historical geochemical relationships; and (iv) compare the information provided by HGRFs with that obtained from conventional sediment assessment indices.

2. Material and methods

2.1. Sampling

Sampling was conducted in December 2023 within the Sacca di Goro (Fig. 1). Sediment collection was performed from a boat using a manually operated Van Veen grab sampler deployed at each sampling station. The upper 0–5 cm of sediment was collected at each site, and approximately 1 L of sediment was recovered per sample. The collected sediment was transferred into appropriately labelled polyethylene bags for transport and storage. Quality Assurance and Quality Control (QA/QC): to prevent cross-contamination during sediment sampling, the Van Veen grab was thoroughly rinsed by immersion in water after each collection to remove any residual material from the previous sample. Immediately after collection, the sediment samples were placed in a portable refrigerator maintained at 4 °C and kept under refrigerated conditions throughout transport to the laboratory. Upon arrival, the samples were immediately transferred to a refrigerator and stored at 4 °C until analysis (EPA, 2001).

To perform different analytical techniques samples were manually quartered to obtain two representative aliquots, including one for grain-size and one for geochemical analyses, respectively. Samples collected as part of this study will hereinafter be referred to as recent samples (RS).

2.2. Textural analyses

Organic matter was first removed by subjecting each sample aliquot to oxidation with a 16% (v/v) H_2O_2 solution (Edwards, 2002). The treatment was continued until all visible effervescence had ceased, indicating complete oxidation of organic matter.

Following organic matter removal, the sediment was separated into sandy and pelitic fractions by wet sieving through a 63 μm mesh sieve. The sandy fraction retained on the sieve was collected in appropriately sized beakers and oven-dried at 105 °C for 24 h. After drying, the beakers were transferred to a desiccator containing granular silica gel (Carlo Erba Reagents, Val de Reuil Cedex, France) and allowed to cool to room temperature prior to weighing, ensuring accurate determination of dry mass. The dry weight of the sandy fraction was subsequently recorded for each sample.

The pelitic fraction (<63 μm) was collected in 5 L jugs and left to settle for approximately 72 h, until complete sedimentation was achieved, as indicated by the clarification of the supernatant. This latter was then carefully siphoned off, avoiding resuspension of the settled material. For each sample, a 0.60 ± 0.05 g subsample was withdrawn for particle-size analysis to determine the relative proportions of silt and clay. Measurements were performed using a Mastersizer 3000 laser diffraction particle size analyser (Malvern Panalytical Ltd., Malvern, UK).

The remaining pelitic material was transferred into appropriately sized beakers, and its wet weight was recorded prior to oven-drying at 105 °C for 72 h. After drying, the samples were cooled in a desiccator and weighed to determine their dry mass. The dry weight corresponding to the aliquot removed for particle-size analysis was estimated using the wet-to-dry weight ratio calculated for each sample (American Society for Testing and Materials ASTM, 1996).

The resulting data were used to calculate the relative abundances of sand, silt, and clay within each sediment sample. The sandy fraction corresponded to particles >63 μm, whereas the pelitic fraction (<63 μm) was further subdivided into silt and clay fractions according to the particle-size distribution obtained by laser diffraction.

2.3. Geochemical analyses

Each aliquot designated for compositional analyses was subjected to repeated washing cycles using ultrapure deionized water (18.2 MΩ·cm) produced by an Arium® Mini UV purification system (Sartorius Lab Instruments GmbH & Co. KG, Göttingen, Germany). The washing procedure was performed to remove residual soluble salts associated with lagoon water entrained within the sediment matrix and to minimize potential chloride-related interferences during geochemical analyses (Loring and Rantala, 1992). During each washing cycle, the sediment was re-suspended in deionized water and allowed to settle for 72 h at 4 °C until a clear supernatant was obtained. This latter was then carefully siphoned off, avoiding resuspension of the settled material and replaced with fresh deionized water. Washing cycles were repeated until the electrical conductivity of the supernatant decreased to ≤ 400 μS cm^{-1}, determined through a HI-98331 conductivity tester (Hanna Instruments, Smithfield, RI, USA), a value comparable to that typically observed in freshwater conditions (Rusydi, 2018).

Following desalination, the sediment subsamples were dried in an oven at 50 °C until complete removal of interstitial water. The dried sediments were then homogenized using an RS 200 Vibratory Disc Mill (Retsch GmbH, Haan, Germany) until a fine, homogeneous powder was obtained. QA/QC: to minimize the risk of cross-contamination, the grinding equipment was thoroughly cleaned between samples using compressed-air cleaning, water washing, and denatured ethyl alcohol rinsing of all sample-contact surfaces. Prior to each grinding cycle, the system was conditioned using an aliquot of the sample to be processed, which was subsequently discarded (Thompson and Bankston, 1970; Hickson and Juras, 1986).

Subsequently, the Loss on Ignition (LOI) analyses was performed: for each subsample, an aliquot of 0.60 ± 0.05 g was weighed using a precision balance (Denver Instrument® GmbH, Göttingen, Germany) and transferred into pre-weighed ceramic crucibles. LOI was determined by heating the samples in a muffle furnace to 1000 °C at a heating rate of 3 °C min^{-1} and maintaining this temperature for 8 h. Following ignition, the crucibles were allowed to cool gradually inside the furnace to approximately 180 °C and were subsequently transferred to a desiccator containing granular silica gel (Carlo Erba Reagents, Val de Reuil Cedex, France) until room temperature was reached, thereby minimizing atmospheric moisture uptake. The crucibles were then reweighed, and LOI values were calculated from the mass loss during ignition. The LOI data were subsequently integrated with the major-oxides composition. QA/QC: prior to use, all crucibles were heated at 550 °C for 1 h (Majlesi et al., 2021) and subsequently cooled in a desiccator before weighing.

The spatula used for sample handling was cleaned with denatured ethyl alcohol between successive samples (American Society for Testing and Materials ASTM, 2000).

For the determination of major-oxide and trace-element contents, an aliquot (4.0 ± 0.5 g) of each powdered subsample was pressed into boric acid–bound pellets using a benchtop hydraulic press (PP25, Retsch GmbH, Haan, Germany). QA/QC: to prevent cross-contamination by dust generated during the processing of different samples, each produced pellet was immediately stored in a sealed plastic bag until analysis. To minimize contamination during sample preparation, all tools were cleaned with denatured ethyl alcohol and compressed air between successive samples (American Society for Testing and Materials ASTM, 2000).

Major-oxide and trace-element contents were determined by wavelength-dispersive X-ray fluorescence spectrometry (WD-XRF) using an ARL Advant'XP+ spectrometer (Thermo Fisher Scientific Inc., Waltham, MA, USA). Major-oxides were expressed as weight percent (wt%), including SiO_2, TiO_2, Al_2O_3, Fe_2O_3, MnO, MgO, CaO, Na_2O, K_2O, and P_2O_5. Trace-element contents were determined as mg kg^{-1} and included Pb, Zn, Cu, V, Ni, and Cr. QA/QC: analytical accuracy and precision were evaluated through triplicate measurements of the certified reference materials (stream sediment powders) JSd-1, JSd-2 and JSd-3 (Geological Survey of Japan, Tsukuba, Japan). The analytical results obtained for the reference materials are reported in the Supplementary Materials (Tables S1–S3). Detection limits (LOD) for the analyzed elements were previously established for the same instrument by Barbero et al. (2021) and Saccani et al. (2022): LOD for major-oxides were 0.05 wt% for SiO_2 and MnO, 0.04 wt% for CaO, 0.10 wt% for Fe_2O_3, and 0.01 wt% for all remaining major-oxides. LOD for trace-elements were ≤ 5 mg kg^{-1} for all analyzed trace-elements. Peak intensity processing and matrix-effect corrections were performed according to the procedure of Lachance and Traill (1966).

2.4. Development of a site-specific geochemical reference

A set of historical sediment data collected during 2003, 2004, and 2005 was selected as the reference framework, following mentioned as historical dataset (HD). The HD was originally produced within environmental monitoring activities coordinated by the Province of Ferrara (2007) and comprised 95 surface-sediment samples collected during four surveys conducted in September 2003 (n = 20), July 2004 (n = 25), November 2004 (n = 25), and June 2005 (n = 25). These observations corresponded to 25 unique spatial sampling stations distributed across the Sacca di Goro (Fig. 1). Twenty stations were repeatedly sampled during all four historical surveys, whereas the remaining five stations were sampled during the three surveys conducted from July 2004 to June 2005. Available data for the HD were:

- Grain-size data, available for 50 of the 95 samples, collected during the November 2004 and June 2005 surveys.
- Major-oxide compositions (SiO_2, TiO_2, Al_2O_3, Fe_2O_3, MnO, MgO, CaO, Na_2O, K_2O, and P_2O_5), LOI, and trace-element contents (Pb, Zn, Cu, V, Ni, and Cr), available for all 95 samples.

The HD covered the main western, central, and eastern sectors of the Sacca di Goro, including its southern sector, thereby providing repeated spatial coverage of the Sacca di Goro. Owing to its spatial coverage, sample density and multi-campaign design, the HD represents the most comprehensive geochemical dataset currently available for the Sacca di Goro prior to the 2023 survey conducted as part of this study. An additional advantage of the HD is its analytical comparability with the present investigation. Major-oxide and trace-element contents were determined using the same WD-XRF analytical methodology adopted in this study, thereby minimizing potential biases associated with analytical procedures and inter-laboratory variability.

2.4.1. Statistical analysis of sedimentological and geochemical relationships in the historical dataset

All statistical analyses and graphical outputs were produced using RStudio (version 2026.01.0-392 – http://www.posit.co/ - Posit PBC, Boston, USA) and QGIS (Version 3.44.6).

To assess the spatial comparability between the historical and recent surveys, the 25 unique historical sampling stations and the 20 stations of the RS were compared spatially. In QGIS, the convex hull of the HD was used to define the spatial domain covered by the historical survey, and the proportion of recent stations falling within this domain was calculated. Nearest-neighbour distances between recent and historical stations were also calculated.

In RStudio, the internal consistency of the HD was assessed by comparing the 2003, 2004, and 2005 surveys. Differences among sampling campaigns were evaluated using Kruskal–Wallis tests on major-oxides, LOI, and trace-element contents. In addition, the distributions of the measured variables were visually inspected to assess the degree of overlap among survey years before combining the data.

To investigate the relationships between sediment texture, major-oxide compositions and trace-element distributions, statistical analyses were performed. Only samples for which both grain-size and geochemical data were available were considered in this phase of the study. Consequently, these analyses were restricted to the 50 samples for which grain-size data were available, hereafter referred to as the historical subset (HS). The analyzed variables included all grain-size data, major-oxide, LOI and trace-element contents.

Relationships among variables were investigated using Spearman's rank correlation coefficient (ρ), given the non-normal distribution of most variables, assessed using the Shapiro-Wilk test. A correlation matrix was calculated using pairwise complete observations and visualized through hierarchical clustering heat maps.

The correlation analysis was used as an exploratory step to identify potential geochemical and sedimentological associations and to identify candidate lithogenic proxies for subsequent evaluation.

2.4.2. Principal component analysis

Principal Component Analysis (PCA) was performed on the HS (n = 50) to explore the main sedimentological and geochemical associations and to identify groups of variables sharing common controls.

The PCA included all grain-size data, major-oxide, LOI, and trace-element contents available for the HS. Prior to the analysis, all variables were standardized to zero mean and unit variance to remove the influence of differences in contents ranges and measurement units (Srivastava et al., 2024).

Grain-size fractions were intentionally included in the PCA to evaluate the relative importance of sediment texture and geochemical composition in controlling trace-element distributions and to support the identification of candidate lithogenic proxies.

2.4.3. Selection of lithogenic proxies and development of HGRFs

To identify the most suitable lithogenic proxies for each trace-element, candidate proxies were first identified from the sedimentological and geochemical relationships observed in the HS, based on the results of the Spearman correlation analysis and PCA. The subsequent quantitative evaluation of candidate proxies was performed using the HD (n = 95), for which major-oxide and trace-element data were available for all samples.

Simple linear regression models were fitted using each candidate major-oxide proxy as the independent variable and the corresponding trace-element contents as the dependent variables. Model performance was assessed using the adjusted coefficient of determination (adj. R^2), as a measure of the explanatory power of each candidate proxy. Because all models compared for a given trace-element were fitted using the same number of observations and included a single predictor, the adj. R^2 values were directly comparable among candidate proxies. The statistical comparison was interpreted in conjunction with the

sedimentological and geochemical relationships identified in the HS, so that proxy selection considered both the explanatory performance of the regression models and the consistency of the selected proxy with the observed sedimentological and geochemical controls.

Following the selection of the lithogenic proxies, HGRFs were developed using the HD. To characterize the relationship between trace-elements and their respective lithogenic proxies, robust linear regression models were fitted using the Least Trimmed Squares (LTS) estimator. This approach was selected to reduce the influence of potential outliers and extreme observations that may affect the estimation of regression coefficients in environmental datasets. Robust regressions were performed in RStudio using the "ltsReg function" implemented in the "robustbase package". The default trimming proportion was adopted.

For each trace-element, the relationship with the selected proxy was described by the following equation (Eq.1):

$$C_i = a + bX \quad (1)$$

where "C_i" is the content of the trace-element i, "X" is the content of the selected lithogenic proxy, "a" is the intercept, and "b" is the slope coefficient. Model performance was evaluated using the adj. R^2.

To assess whether trace-element contents differed from the values predicted by the HGRFs, residuals were calculated for each sampling location as the difference between observed and HGRF-predicted contents. The spatial structure of the residuals was then evaluated using empirical semivariograms calculated from the UTM coordinates of the sampling locations (Beguería and Pueyo, 2009). Variograms were calculated and fitted using the "gstat package" in RStudio, and the resulting spatial ranges were used to account for spatial dependence in the subsequent analysis. This approach is consistent with established applications of generalized least-squares (GLS) models to spatially correlated environmental and soil data (Beguería and Pueyo, 2009; Beguería et al., 2013). For each element, the mean residual was subsequently evaluated using a GLS model with a spherical spatial correlation structure, implemented with the "nlme package" and fitted by restricted maximum likelihood (REML). The spatial range was fixed to the value obtained from the corresponding variogram because of the limited number of recent samples (n = 20). Positive mean residuals indicated trace-element contents higher than those predicted by the historical relationships, whereas negative values indicated lower contents. The spatial structure of the fitted models was checked using Moran's I on the normalized residuals. P-values were adjusted for multiple comparisons using the Holm procedure, with adjusted p-values < 0.05 considered statistically significant.

Furthermore, to evaluate whether individual samples remained consistent with the historical conditions, an empirical reference variability envelope was constructed for each HGRF. The purpose of the envelope was to characterize the site-specific range of trace-element variability observed under the historical conditions. Accordingly, the envelope describes the empirical historical variability around the HGRF and does not quantify the uncertainty associated with the fitted regression. The empirical distribution of the residuals from the LTS regression was therefore used to define the reference range. For each sample in the HD, the residual was calculated as the difference between the observed trace-element content and the value predicted by the corresponding LTS regression. The 2.5th and 97.5th percentiles of the empirical residual distribution were used to define the lower and upper bounds of the envelope, respectively, by adding these values to the HGRF-predicted content. The resulting envelope represents the central 95% of the empirical residual variability observed in the historical dataset.

2.5. Comparison with conventional sediment assessment indices

To provide a direct comparison between the HGRF approach and conventional sediment assessment methods, the EF (Abrahim and Parker, 2007), Igeo (Müller, 1969), CF (Hakanson, 1980), and PLI (Tomlinson et al., 1980) were calculated for Pb, Zn, Cu, V, Ni and Cr. The indices were calculated for both the HD and RS.

The lithogenic proxies were selected according to the proxy-selection criteria described in Section 2.4.3 and consistently applied to the investigated elements. Regional reference values were obtained from Migani et al. (2015). Differences between the historical and recent datasets were evaluated descriptively using the median and interquartile range.

3. Results

3.1. Characterization of recent samples

The results of the grain-size characterization, major-oxide compositions, and trace-element contents for RS in the Sacca di Goro are reported in Tables S4, S5, and S6 of the Supplementary Materials, respectively.

3.2. Internal consistency of the historical dataset

The HD comprised 95 observations collected at 25 unique spatial stations, whereas the RS included 20 stations. 17 of the 20 recent stations (85%) fell within the convex hull defined by the historical sampling network (Fig S1 – Supplementary Materials). For the 2023 stations, the distance to the nearest historical station ranged from 148 m to 794 m, with a median of 465 m and a mean of 457 m. Conversely, the distance from historical stations to the nearest recent station ranged from 148 m to 1394 m, with a median of 541 m and a mean of 618 m.

Temporal differences among the 2003, 2004 and 2005 surveys were evaluated to verify the internal consistency of the HD through Kruskal–Wallis tests performed on major-oxide, LOI and trace-element contents. Results revealed no systematic inter-annual differences. Visual inspection of the distributions further confirmed the substantial overlap among survey years (Fig. 2), supporting the aggregation of the monitoring campaigns from 2003, 2004, and 2005 into a single HD.

3.3. Relationships between sediment texture, major-oxides and trace-elements in historical samples

Spearman correlation analysis performed on the HS revealed strong relationships among sedimentological and geochemical variables (Fig. 3).

Sand was strongly positively correlated with SiO_2 and Na_2O, and negatively correlated with Al_2O_3, K_2O and LOI. Conversely, clay showed positive correlations with Al_2O_3, K_2O, LOI, Pb, Zn, Cu, and V.

Strong positive correlations ($\rho > 0.8$) were observed among Pb, Zn, Cu and V. These elements were also positively correlated with Al_2O_3, Fe_2O_3, TiO_2 and K_2O, whereas negative correlations were observed with sand, SiO_2 and Na_2O.

Ni showed positive correlations with Zn, Cu, V, Al_2O_3, K_2O, Fe_2O_3 and clay, while negative correlations were observed with sand, MgO and CaO.

Regarding Cr, correlations with Pb, Zn, Cu and V were lower than those observed among the other trace-elements ($\rho < 0.5$). The strongest positive correlations were observed with TiO_2, Fe_2O_3 and Ni, whereas correlations with grain-size fractions were comparatively weak.

PCA highlighted that the first two principal components (PC1, PC2) accounted for 77.0% of the total variance, with PC1 and PC2 explaining 62.4% and 14.6%, respectively (Fig. 4).

PC1 was characterized by positive loadings of Sand, Na_2O and SiO_2, and negative loadings of Al_2O_3, Cu, Clay, V, K_2O, Zn and Fe_2O_3. Pb, LOI and Ni also showed negative loadings along this component. In the variable factor map (Fig. 4), Sand, SiO_2 and Na_2O clustered on the positive side of PC1, whereas Clay, Al_2O_3, K_2O, LOI and most trace-elements were grouped on the negative side.

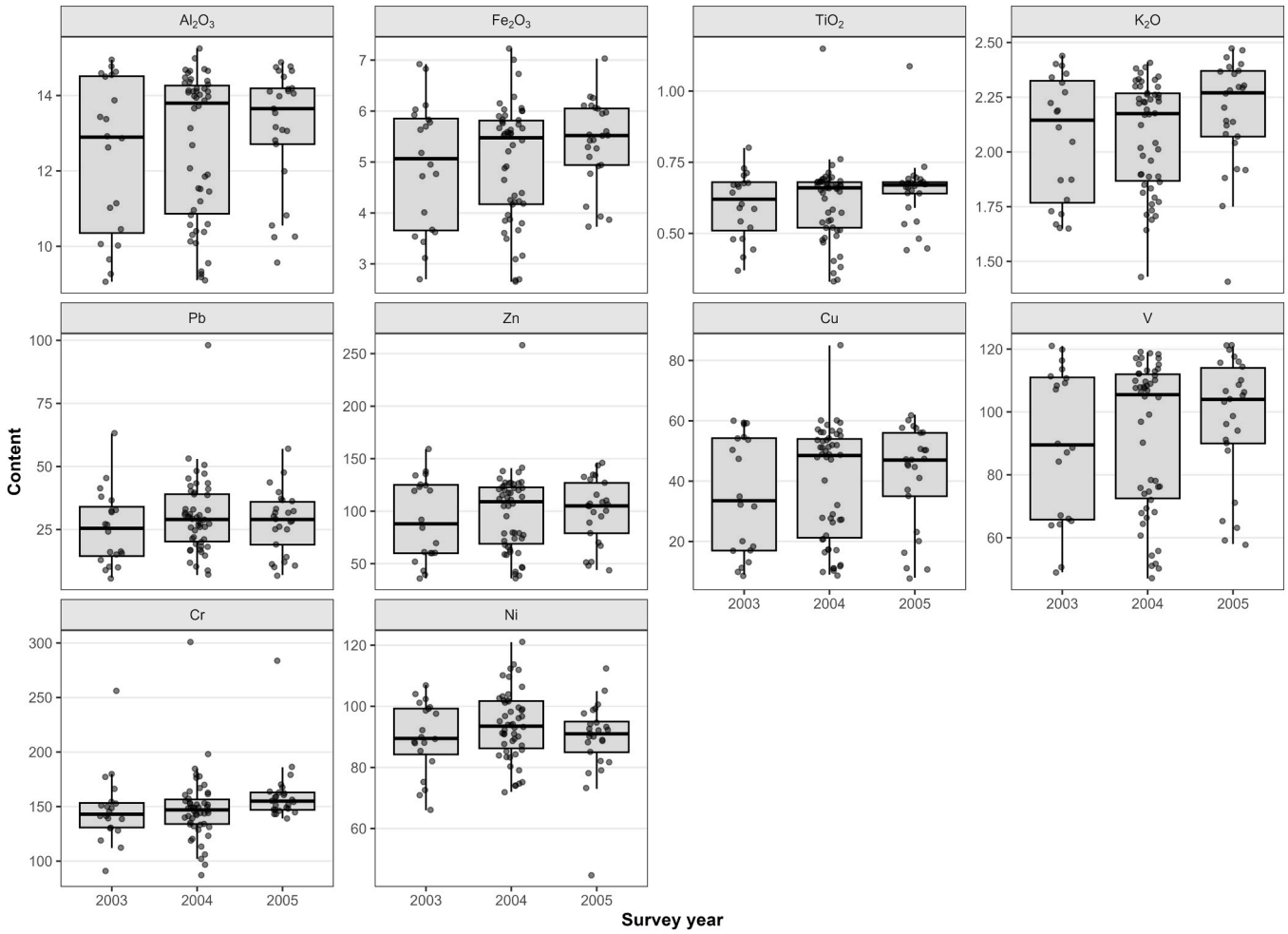


Fig. 2. Distribution of selected major-oxides (wt%) and trace-elements (mg kg^{-1}) in the HD (Province of Ferrara, 2007).

PC2 was dominated by Cr, TiO_2, P_2O_5, MnO and Fe_2O_3. MgO and CaO also showed positive loadings on this component, while Ni displayed a negative loading. Cr was associated with TiO_2, MnO, and P_2O_5.

3.4. Development of HGRFs

Among the lithogenic proxies, Al_2O_3 generally provided the highest explanatory power for trace-element contents. It yielded the strongest relationships for Cu (adj. $R^2 = 0.92$) and V (adj. $R^2 = 0.91$), and also produced higher adjusted R^2 values than K_2O for Zn (0.77 vs. 0.69) and Pb (0.48 vs. 0.43). Ni represented the only exception, with comparable explanatory power obtained using K_2O (adj. $R^2 = 0.60$) and Al_2O_3 (adj. $R^2 = 0.59$), whereas markedly lower values were obtained for the other evaluated proxies.

In contrast, Cr showed a distinctly different behaviour from the other trace elements. The strongest relationship was observed with TiO_2 (adj. $R^2 = 0.70$), whereas substantially lower explanatory power was obtained for Fe_2O_3 (adj. $R^2 = 0.28$) and MnO (adj. $R^2 = 0.13$).

Based on the quantitative comparison performed using the HD and on the sedimentological and geochemical relationship identified in the HS, Al_2O_3 was selected as the reference lithogenic proxy for Pb, Zn, Cu, V, and Ni, whereas TiO_2 was selected for Cr. Although K_2O provided a marginally higher adj. R^2 for Ni (0.60 vs. 0.59) in the HD, the two proxies showed comparable explanatory power. Al_2O_3 was therefore selected for Ni based on its stronger association with the fine-grained sediment fraction identified in the HS, providing additional sedimentological support for its use as lithogenic proxy.

Using the selected proxies, robust LTS regression models were developed to establish HGRFs for the investigated trace-elements (Fig S2 – Supplementary Materials). The resulting equations and model performances are reported in Table 1. Positive slopes were obtained for all models, showing increasing trace-element contents with increasing abundance of the selected lithogenic proxy. The highest slope coefficient was observed for Cr as a function of TiO_2 (160.53), whereas the lowest was obtained for Ni as a function of Al_2O_3 (4.29). These HGRFs were subsequently used to estimate expected trace-element contents and calculate residual values for the assessment of the RS.

3.5. Application of the HGRFs to recent samples

Residual analysis revealed distinct patterns among the investigated trace elements (Fig. 5). Pb, Cu and V showed residuals distributed around zero, with mean residuals of 1.24 mg kg^{-1}, −0.54 mg kg^{-1} and −1.82 mg kg^{-1}, respectively. No significant departures from the HGRF predictions were detected for these three elements.

In contrast, Zn, Ni and Cr showed a predominance of positive residuals, with positive values occurring in 17, 19 and all 20 RS, respectively. Mean residuals were 38.76 mg kg^{-1} for Zn, 35.12 mg kg^{-1} for Ni and 64.96 mg kg^{-1} for Cr. The positive departures for Ni and Cr remained significant after correction for multiple comparisons (Holm-adjusted $p < 0.01$ and <0.001, respectively), whereas the positive departure observed for Zn did not reach the significance threshold after correction ($p = 0.056$). Cr showed the largest mean departure from the historical relationships.

No significant spatial autocorrelation was detected in the normalized GLS residuals for any of the investigated elements (Moran's I, $p > 0.05$),

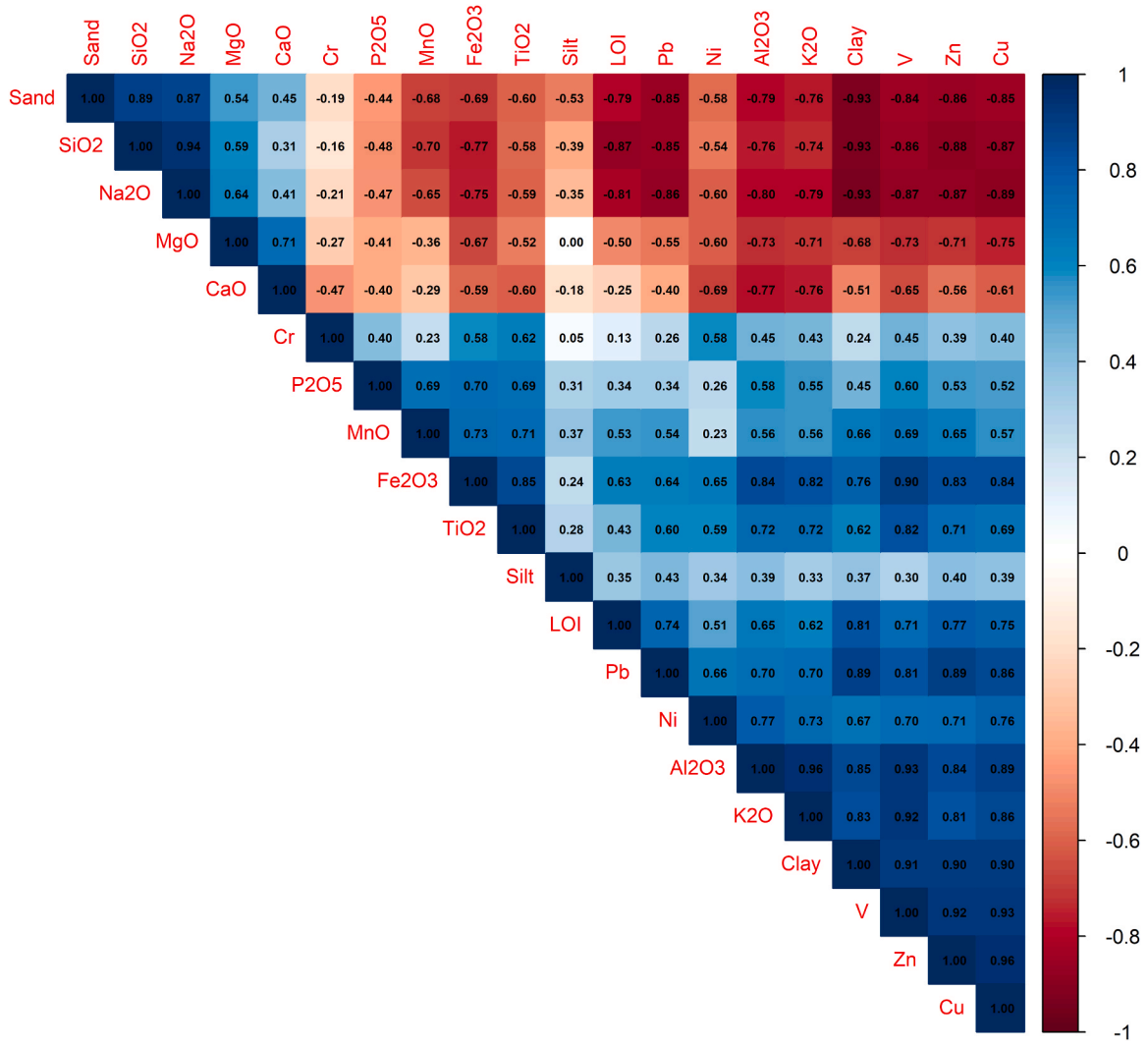


Fig. 3. Spearman correlation matrix including grain-size, major-oxides and trace-elements data, calculated using the HS. Correlation coefficients (ρ) are displayed within each cell and colour-coded according to their magnitude and direction. The color scale indicates the ρ, with values ranging from −1 (blue − negative correlation) to +1 (red − positive correlation). Variables are ordered using hierarchical clustering based on correlation similarity.

indicating that no significant residual spatial structure remained after accounting for spatial dependence in the GLS models.

The systematic nature of these departures was further evaluated by comparing the RS with a reference variability envelope defined for each HGRF (Fig. 6): approximately 65% of the 2023 samples for Zn, 90% for Ni, and 70% for Cr exceeded the upper limit of their respective variability envelope.

3.6. Conventional sediment assessment indices

The conventional sediment indices were calculated using the regional reference values reported by Migani et al. (2015). Based on the evaluation of the lithogenic proxies described above, Al_2O_3 was selected as the normalizing proxy for Pb, Zn, Cu, V and Ni, whereas TiO_2 was selected for Cr. The corresponding reference contents were 13.75 wt% for Al_2O_3 and 0.60 wt% for TiO_2, while for the target elements were: 17 mg kg^{-1} for Pb, 87 mg kg^{-1} for Zn, 30 mg kg^{-1} for Cu, 96 mg kg^{-1} for V, 118 mg kg^{-1} for Ni and 169 mg kg^{-1} for Cr. The same reference values and element-specific proxy associations were applied to both HD and RS.

The median values, ranges and corresponding classification classes for EF, Igeo, CF and PLI are reported in Tables S7–S10 – Supplementary materials. For EF, the median values of all six elements fell within the minimal enrichment class in both HD and RS. Pb showed the highest median EF in both datasets (1.71 in HD and 1.88 in RS), while median EF values for Ni and Cr increased from 0.83 and 0.85 in HD to 1.15 and 1.26 in RS, respectively; all median values remained within the minimal enrichment class.

For Igeo, the median values for Pb and Cu fell within the unpolluted to moderately polluted class in both HD and RS. Zn was classified as unpolluted in HD (median Igeo = −0.31) and as unpolluted to moderately polluted in RS (0.22). The median Igeo values for V, Ni and Cr remained within the unpolluted class in both datasets.

For CF, the median values for Pb, Zn, Cu and V corresponded to moderate contamination in both HD and RS. Ni and Cr were classified as showing low contamination in HD, with median CF values of 0.78 and 0.88, respectively, whereas their median values in RS were 1.11 and 1.27, respectively, corresponding to moderate contamination.

The median PLI was 1.19 in HD and 1.43 in RS, with both datasets falling within the polluted category.

4. Discussion

4.1. Reliability of the historical dataset

The spatial distribution of the RS was broadly consistent with that of the HD. Despite the lower number of stations, the RS covered the main

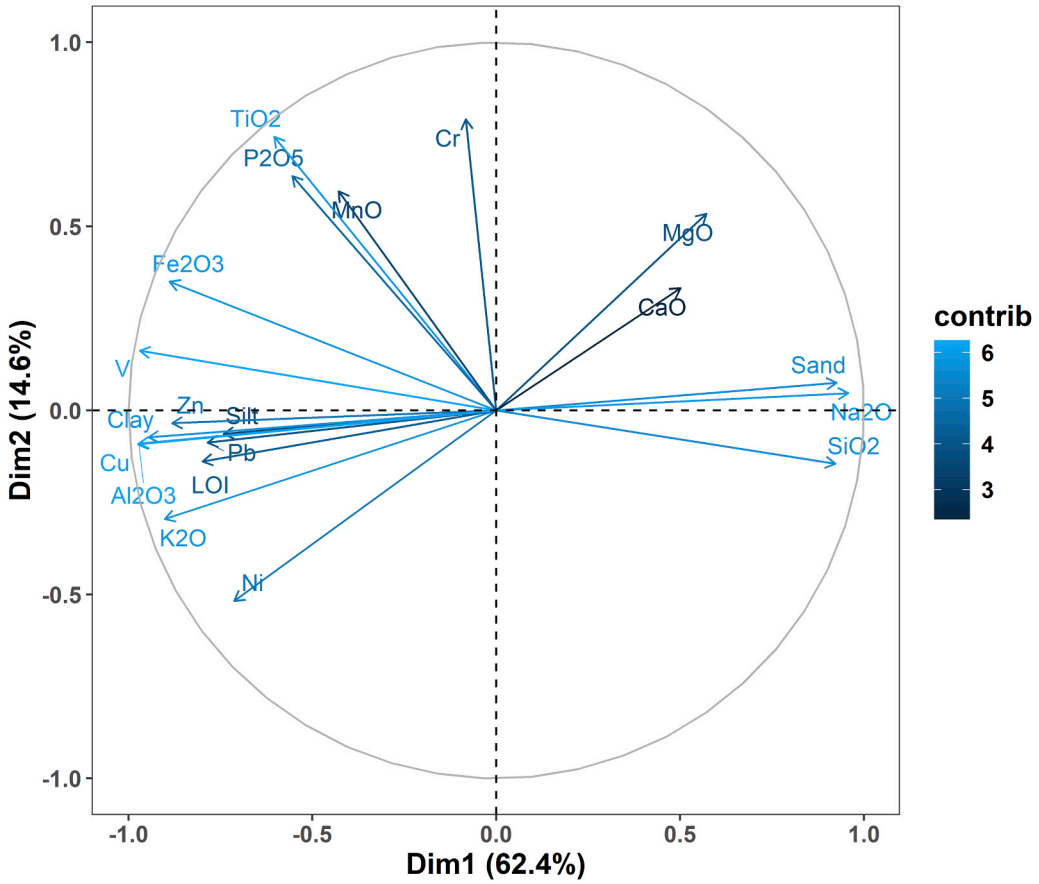


Fig. 4. Principal Component Analysis (PCA) loading plot based on sedimentological, major-oxides and trace-elements data for the HS. The color scale indicates the contribution (%) of each variable to the definition of the displayed principal components, with darker colors corresponding to lower contributions and lighter colors to higher contributions.

Table 1
HGRFs established from the HD using robust LTS regression. For each trace-element, the selected proxy, reference equation and Adj. R^2 are reported.

Element	Proxy	Equation	Adj. R^2
Pb	Al_2O_3	$Pb = -31.07 + 4.54 \cdot Al_2O_3$	0.48
Zn	Al_2O_3	$Zn = -110.17 + 16.15 \cdot Al_2O_3$	0.77
Cu	Al_2O_3	$Cu = -77.07 + 9.10 \cdot Al_2O_3$	0.92
V	Al_2O_3	$V = -62.41 + 12.14 \cdot Al_2O_3$	0.91
Ni	Al_2O_3	$Ni = 37.47 + 4.29 \cdot Al_2O_3$	0.59
Cr	TiO_2	$Cr = 47.81 + 160.53 \cdot TiO_2$	0.70

areas previously investigated, with most stations located within the HD domain. The few stations falling outside this domain were nevertheless located relatively close to historical sampling locations. Therefore, the observed differences are unlikely to be explained solely by differences in spatial coverage. Although the two sampling networks were not identical, their overall spatial correspondence supports the use of the RS for comparison with the HD.

Sediment texture generally represents one of the main controls on trace-element contents (Bábek et al., 2015; Matys Grygar and Popelka, 2016), making the assessment of sedimentological comparability a prerequisite for evaluating differences in geochemistry between the HD and RS. The Shepard sediment classification method (Shepard, 1954) indicates a substantial overlap between the HS and RS (Fig. 7). Both sampling campaigns include sediments belonging to the same major textural classes, namely sand, silty sand, sandy silt and clayey silt. Although clay-rich sediments are more abundant in the HS, RS fall entirely within the textural variability previously documented, supporting the validity of the temporal comparison.

Comparison of major-oxide compositions indicates that the RS fall within the compositional range defined by the HD (Table 2). In particular, TiO_2, Al_2O_3 and Fe_2O_3 contents show comparable central tendencies and ranges between periods, while the observed variability remains largely encompassed by the distribution in the HD. Although K_2O contents are generally higher in the RS, the overall major-oxide compositions indicate that these latter broadly belong to the same geochemical population represented by the HD.

4.2. *Lithogenic controls and historical conditions*

Correlation matrix and PCA suggest that sediment texture and mineralogical composition are the main controls on trace-element distributions in the historical conditions of the Sacca di Goro. Pb, Zn, Cu and V are associated with the fine-grained aluminosilicate fraction, indicating a strong grain-size control on their distribution (Bábek et al., 2015), with Fe-bearing phases possibly contributing through adsorption and co-precipitation (Horowitz, 1991). Ni was primarily associated with the aluminosilicate fraction but exhibited weaker lithogenic relationships than Pb, Zn, Cu and V, suggesting that additional controls may contribute to its distribution. The Cr–TiO_2 relationship likely reflects the co-occurrence of Cr-bearing and Ti-bearing heavy minerals concentrated by sedimentary processes within the lagoon. Indeed, sediments derived from the Po River catchment are known to be naturally enriched in trace-elements owing to the lithological characteristics of their source areas (Amorosi et al., 2002; Picone et al., 2008; Bianchini et al., 2012). Elevated Cr contents have been attributed to the occurrence of spinel-group minerals, while serpentinite-derived detritus and associated heavy-mineral assemblages, including garnet, epidote, pyroxene,

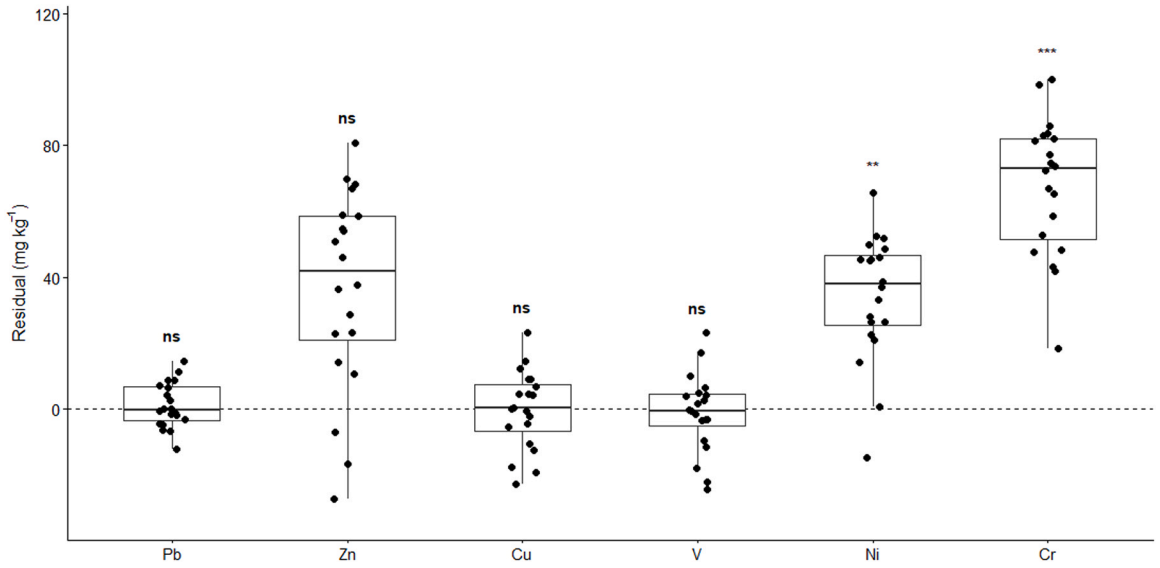


Fig. 5. Distribution of residuals between observed and HGRF-predicted trace-element contents in the recent samples (RS). Boxplots show the median, interquartile range and overall distribution of residuals, with individual points representing the 20 sampling locations. The dashed horizontal line indicates zero departure from the historical relationships. Significance levels refer to the spatial GLS models after Holm correction for multiple comparisons: ns, not significant; $^{**}p < 0.01$; $^{***}p < 0.001$.

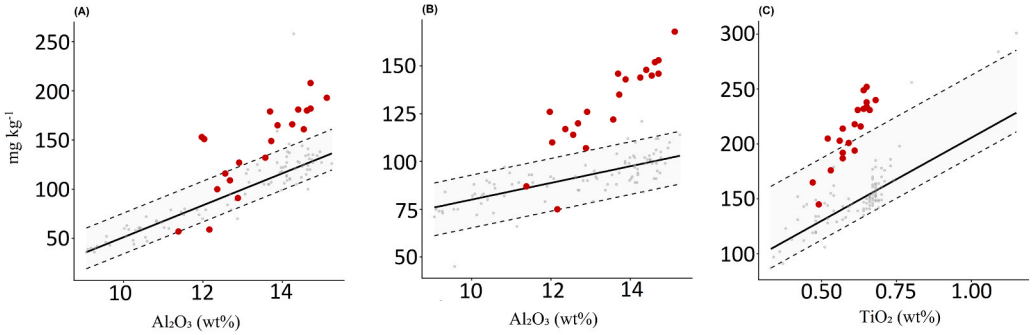


Fig. 6. HGRFs between Zn and Al_2O_3 (A), Ni and Al_2O_3 (B), and Cr and TiO_2 (C) for sediments from the Sacca di Goro. Grey symbols represent samples from HD, whereas red symbols represent RS. Solid lines indicate robust regression models, while dashed lines and shaded areas denote the variability envelope.

hornblende and olivine, have been identified as important carriers of both Cr and Ni (Gazzi and Zuffa, 1970; Gazzi et al., 1973; Bonifacio et al., 2010; Greggio et al., 2017).

The HGRFs developed in this study represent empirical relationships between trace-element contents and their dominant lithogenic proxies within the Sacca di Goro in the reference period. In this light, they should not be interpreted as background functions in the sense of Bábek et al. (2015) and Matys Grygar and Popelka (2016). Indeed, comparison with the regional background values proposed by Migani et al. (2015) shows that contents of some elements, particularly Pb, Zn and Cu, were already higher than the proposed background contents (Table S11 – Supplementary Materials). Rather, the HGRFs describe the geochemical relationships that characterized the Sacca di Goro in the 2003, 2004 and 2005. Therefore, HGRFs provide a site-specific historical reference. By incorporating the effects of sediment texture and composition, these functions allow departures from the historical geochemical conditions of the lagoon to be evaluated independently of grain-size-related variability.

4.3. Trace-element distributions and interpretation of geochemical departures

Among the investigated elements, Ni and Cr showed the most systematic departures from the historical conditions. Both elements yielded significant positive residuals, indicating contents higher than those predicted by the lithogenic relationships established for the HD. In this context, higher Ni/Al_2O_3 ratios and Ni-Cr contents in the RS, compared to the HD (Fig S3, Fig S4 – Supplementary Materials), suggest that the RS display a greater geochemical affinity with sediment compositions commonly associated with Po-derived material (Bianchini et al., 2012; Greggio et al., 2017; Amorosi, 2012). Although the processes responsible for this departure cannot be resolved unequivocally, the observed departures occur together with an increased similarity to sediment populations associated with Po-derived material. Previous investigations of sediments and soils from the Po Plain have shown that Ni and Cr are predominantly associated with lithogenic mineral phases and may exhibit limited bioavailability despite relatively high total contents (Sammartino, 2004), indicating that their contents may have a substantial geogenic component. This does not exclude potential environmental relevance, however. Studies conducted in lagoons of the Po Delta have shown that a substantial fraction of Ni may be associated with reducible Fe–Mn oxyhydroxides, indicating that its partitioning and potential mobility may vary according to sediment geochemical conditions (Zonta et al., 2019). The HGRF departures therefore identify Ni and Cr as elements deserving further investigation of mineralogical associations, partitioning, speciation and bioavailability, rather than

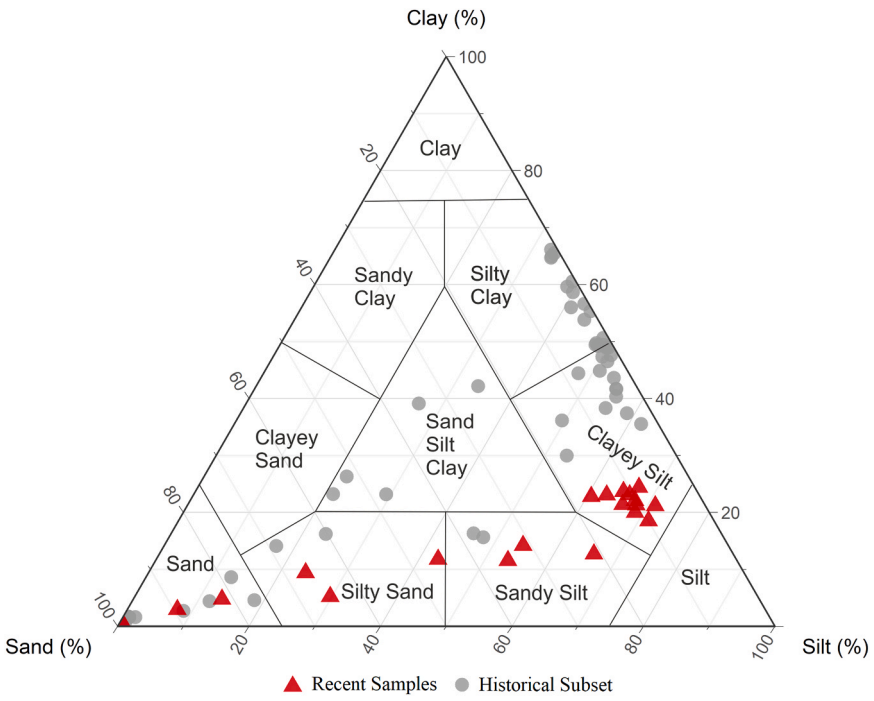


Fig. 7. Shepard sediment classification diagram (Shepard, 1954) showing the distribution of sediment samples from the HS and the RS within the Sacca di Goro.

Table 2
Summary statistics of major-oxide contents (wt%) in the HD and in the RS from the Sacca di Goro. P95 denotes the 95th percentile.

	HD (Province of Ferrara, 2007)				
	SiO_2	TiO_2	Al_2O_3	Fe_2O_3	K_2O
Average	49.58	0.62	12.74	5.08	2.10
Median	47.66	0.66	13.49	5.43	2.18
Max	61.55	1.15	15.25	7.23	2.47
Min	41.59	0.33	9.06	2.65	1.41
P95	60.34	0.73	14.77	6.76	2.40
			RS		
	SiO_2	**TiO_2**	**Al_2O_3**	**Fe_2O_3**	**K_2O**
Average	51.72	0.60	13.41	4.84	2.53
Median	52.38	0.61	13.57	4.84	2.55
Max	55.51	0.68	15.12	6.11	2.89
Min	45.00	0.47	11.38	3.30	2.11
P95	53.10	0.66	14.73	5.73	2.84

constituting evidence of ecological risk themselves (Koukina et al., 2017; Monte et al., 2025).

Zn displayed a distinct pattern compared with the other investigated trace elements. Although positive residuals were observed in 17 of the 20 RS samples, the mean positive departure did not remain statistically significant after accounting for spatial dependence and multiple comparisons. Nevertheless, the predominance of positive residuals suggests a tendency toward higher Zn contents than predicted by the historical relationships. Unlike Ni and Cr, whose departures can be discussed within a provenance-related framework, the positive tendency observed for Zn was not accompanied by comparable departures in Pb and Cu, despite the strong geochemical relationships linking these elements in the HD.

Considering that the study area is subject to intensive shellfish farming activities and frequent ship traffic, these environmental pressures may represent possible contributors to the positive tendency observed for Zn. Zn-based sacrificial anodes, widely used for the cathodic protection of vessels and marine infrastructures, have been recognized as a potential source of Zn in coastal environments (Bird et al., 1996; Rousseau et al., 2009). Agricultural inputs may also contribute, given the extensive cultivation in the upstream drainage basin and surrounding areas (Fig. 1). The use of Zn-containing fertilizers can promote Zn accumulation in agricultural soils (Van et al., 2024), with subsequent mobilization through surface runoff and drainage networks potentially providing an additional pathway to the lagoon. However, given that the Zn departure did not reach statistical significance after correction for multiple comparisons and that the present dataset does not include source-specific tracers, the relative contribution of these potential inputs cannot be established. Continued monitoring would therefore be useful to determine whether the observed Zn pattern persists over time. If confirmed by future observations, Zn stable isotope analyses could provide a complementary approach for investigating its origin and distinguishing among potential natural and anthropogenic sources (Araújo et al., 2017).

4.4. Comparison of geochemical assessment approaches

The conventional sediment assessment indices showed a broadly similar geochemical status for HD and RS relative to the regional reference proposed by Migani et al (Migani et al., 2015). EF values indicated minimal enrichment for all investigated elements in both datasets, while Igeo showed predominantly unpolluted conditions. CF classified Pb, Zn, Cu and V as moderately contaminated in both HD and RS, whereas Ni and Cr were classified as low contamination in HD and moderate contamination in RS. PLI classified both the datasets as polluted. Overall, the comparison with the regional reference therefore indicates a broadly similar geochemical status, with the clearest difference concerning Ni and Cr.

The interpretation of these classifications depends on the reference used to characterize the sediments. The values proposed by Migani et al. (2015). provide a relevant regional benchmark because they derive from a nearby Adriatic setting, although they were not specifically established for the Sacca di Goro. Trace-element contents, however, are also controlled by different factors. Bábek et al. (2015) and Matys Grygar and Popelka (2016) addressed this issue through empirical background functions that describe relationships between trace elements and lithogenic or sedimentological variables, moving beyond the use of fixed background values. A pristine or pre-industrial local reference would

provide the most direct basis for defining natural conditions, but such material can be difficult to identify reliably in coastal systems with long histories of sediment accumulation and anthropogenic influence.

The HGRFs provide a complementary approach by using the historical sediment record of the Sacca di Goro to characterize these geochemical relationships. HD is not assumed to represent pristine or uncontaminated conditions; rather, it provides an empirical reference derived from the system itself. Importantly, the HGRFs do not assign a single fixed background value to each element. Instead, they retain the relationships between trace-element contents and the selected lithogenic proxies represented in the HD, and use these relationships to evaluate the observations in the RS.

The element-specific results illustrate the additional information provided by this approach. Pb, Cu and V were classified as moderately contaminated according to CF in both HD and RS, and no significant HGRFs departures were detected. Ni and Cr were classified as low contamination in HD and moderate contamination in RS, and both showed positive HGRFs departures in RS. Zn showed a more intermediate pattern: CF classified both HD and RS as moderately contaminated, while Igeo classified HD as unpolluted and RS as unpolluted to moderately polluted. Positive HGRFs departures were also observed for Zn, although these were not statistically significant. Thus, the HGRFs provide their clearest additional evidence for Ni and Cr, while the pattern observed for Zn remains suggestive but statistically inconclusive.

The main value of the HGRF approach is therefore to complement conventional sediment indices with a system-specific empirical reference. Repeated application of EF, Igeo, CF and PLI could be valuable for assessing enrichment and contamination relative to a regional benchmark. HGRFs add information that cannot be obtained simply by recalculating these indices using new data. HGRFs use the historical record to characterize the geochemical relationships of the system without requiring a pristine background and without reducing the reference condition to a single fixed elemental value. This can be particularly useful in long-term monitoring programmes, where historical observations can provide an empirical basis for identifying which recent geochemical departures warrant further investigation.

Pristine or pre-industrial sediments would nevertheless remain the most direct reference for characterizing natural background conditions where they can be reliably identified, while empirical background functions offer a more comprehensive approach when sufficient pristine data are available to characterize sedimentological and lithogenic controls (Bábek et al., 2015; Matys Grygar and Popelka, 2016). HGRFs should therefore be considered a complementary alternative for situations in which such references are unavailable or cannot be reliably established. In the present study, the HGRF approach thus provides a means of extracting additional information from historical monitoring data while maintaining a clear distinction between a departure from the historical geochemical relationships and evidence of a specific contamination source or ecological impact.

4.5. Limitations and future perspectives

The main limitation of the present analysis is that the HGRF departures cannot be attributed to specific underlying processes. Although the selected lithogenic proxies account for part of the geochemical variability, the available data do not allow the relative contribution of sediment provenance, mineralogical composition, depositional processes and anthropogenic inputs to be distinguished. Additional sedimentological and mineralogical information would therefore be required to identify the mechanisms responsible for the observed departures.

A further limitation concerns the number of datasets available to define and evaluate the historical relationships. Additional observations covering a wider range of conditions (e.g. different seasons, different wheatear conditions) would allow the robustness of the HGRFs to be tested and their residuals to be evaluated under different circumstances. Future studies could therefore combine HGRFs with detailed information on provenance, grain size, mineralogy and depositional processes, providing a stronger basis for interpreting the causes of possible identified departures.

For the Sacca di Goro, such an integrated approach would be particularly relevant given its ecological importance and its role as a major shellfish-farming area of the northern Adriatic (Tamburini et al., 2022; Summa et al., 2023). It could strengthen the use of HGRFs as a screening framework for identifying geochemical departures and directing subsequent investigations towards their underlying causes and environmental significance.

5. Conclusion

This study demonstrates the value of HGRFs for evaluating recent departures from the geochemical relationships represented by a previous monitoring record. The RS showed a differentiated pattern: Pb, Cu and V remained consistent with the reference relationships, Ni and Cr exhibited significant positive departures, while Zn showed a positive but statistically non-significant pattern after accounting for spatial dependence and multiple comparisons. This element-specific response indicates that the recent dataset does not represent a uniform departure from the established geochemical structure, but rather element-specific departures within the sediment geochemistry.

Conventional indices describe enrichment and contamination relative to a regional reference, whereas HGRFs evaluate whether recent observations remain consistent with the geochemical relationships represented by the earlier dataset. Their distinctive feature is therefore not the assignment of another contamination class, but the use of relationships between trace-element contents and lithogenic controls as the reference itself. This allows recent departures to be interpreted within the geochemical variability documented for the system rather than solely relative to fixed elemental values.

The HD does not represent pristine or uncontaminated conditions, and the HGRFs should not be interpreted as a replacement for a reliable natural background or empirical background functions where these can be established. Their value instead lies in extracting additional information from an existing monitoring record when such references are unavailable or difficult to establish. In this context, the departures identified in the RS represent geochemical signals rather than direct evidence of contamination, source attribution or ecological impact. The HGRF framework therefore adds a system-specific dimension to sediment monitoring by allowing recent observations to be evaluated according to their consistency with the geochemical structure documented by previous observations.

In the Sacca di Goro, the contrasting responses of Pb, Cu, V, Zn, Ni and Cr illustrate how HGRFs can distinguish elements that remain within the established geochemical relationships from those showing recent departures. For Ni and Cr, the positive departures identify these elements as the primary targets for further characterization of mineralogical associations and elemental partitioning, particularly to determine whether the observed differences reflect changes in their association with lithogenic phases and, for Ni, potentially mobile Fe–Mn-bearing phases. The positive pattern observed for Zn, although not statistically significant, suggests that Zn should also be followed in subsequent monitoring. Additional sampling over successive monitoring periods would then allow these patterns to be tested for persistence and recurrence and, where supported by new observations, used to progressively refine the HGRFs. This is particularly relevant for the Sacca di Goro, where improved understanding of changes in sediment geochemistry can contribute to the long-term assessment of a lagoon that supports economically important shellfish production.

Funding

For sampling activities, the authors acknowledge financial support

from PNRR MUR project ECS_00000033 (Ecosystem for Sustainable Transition in Emilia-Romagna (ECOSISTER), CUP: B33D21019790006).

CRediT authorship contribution statement

Antonello Aquilano: Writing – review & editing, Writing – original draft, Visualization, Validation, Software, Methodology, Investigation, Formal analysis, Data curation, Conceptualization. **Joana Buoninsegni:** Writing – review & editing, Formal analysis. **Elena Marrocchino:** Writing – review & editing, Writing – original draft, Supervision. **Carmela Vaccaro:** Supervision, Resources.

Declaration of Competing Interest

The authors declare that they have no known competing financial interests or personal relationships that could have appeared to influence the work reported in this paper.

Acknowledgements

The authors would like to thank Umberto Tessari of the Department of Physics and Earth Sciences at the University of Ferrara for his support in conducting the grain-size analyses.

Appendix A. Supporting information

Supplementary data associated with this article can be found in the online version at doi:10.1016/j.rsma.2026.105474.

Data availability

Data will be made available on request.

References

Abrahim, G.M.S., Parker, R.J., 2007. Assessment of heavy metal enrichment factors and the degree of contamination in marine sediments from Tamaki Estuary, Auckland, New Zealand. Environ. Monit. Assess. 136, 227–238. https://doi.org/10.1007/s10661-007-9678-2.

American Society for Testing and Materials (ASTM), 1996. Standard guide for collection, storage, characterization, and manipulation of sediments for toxicological testing. Annu. Book. ASTM Stand. 05, 805–825.

American Society for Testing and Materials (ASTM). E1391 -94 Standard guide for collection, storage, characterization, and manipulation of sediments for toxicological testing. ASTM Stand. Environ. Sampl., vol. 5, Conshohocken, PA: 2000, p. 768–788.

Amir, M., Paul, D., Samal, R.N., 2019. Sources of organic matter in Chilika lagoon, India inferred from stable C and N isotopic compositions of particulates and sediments. J. Mar. Syst. 194, 81–90. https://doi.org/10.1016/j.jmarsys.2019.03.001.

Amorosi, A., 2012. Chromium and nickel as indicators of source-to-sink sediment transfer in a Holocene alluvial and coastal system (Po Plain, Italy). Sediment. Geol. 280, 260–269. https://doi.org/10.1016/j.sedgeo.2012.04.011.

Amorosi, A., Centineo, M.C., Dinelli, E., Lucchini, F., Tateo, F., 2002. Geochemical and mineralogical variations as indicators of provenance changes in Late Quaternary deposits of SE Po Plain. Sediment. Geol. 151, 273–292. https://doi.org/10.1016/S0037-0738(01)00261-5.

Araújo, D.F., Boaventura, G.R., Machado, W., Viers, J., Weiss, D., Patchineelam, S.R., et al., 2017. Tracing of anthropogenic zinc sources in coastal environments using stable isotope composition. Chem. Geol. 449, 226–235. https://doi.org/10.1016/j.chemgeo.2016.12.004.

Bábek, O., Grygar, T.M., Faměra, M., Hron, K., Nováková, T., Sedláček, J., 2015. Geochemical background in polluted river sediments: How to separate the effects of sediment provenance and grain size with statistical rigour? Catena 135, 240–253. https://doi.org/10.1016/j.catena.2015.07.003.

Barbero, E., Zaccarini, F., Delavari, M., Dolati, A., Saccani, E., Marroni, M., et al., 2021. New evidence for Late Cretaceous plume-related seamounts in the Middle East sector of the Neo-Tethys: Constraints from geochemistry, petrology, and mineral chemistry of the magmatic rocks from the western Durkan Complex (Makran Accretionary Prism, SE Iran). Lithos 396–397, 106228. https://doi.org/10.1016/j.lithos.2021.106228.

Beguería, S., Pueyo, Y., 2009. A comparison of simultaneous autoregressive and generalized least squares models for dealing with spatial autocorrelation. Glob. Ecol. Biogeogr. 18, 273–279. https://doi.org/10.1111/j.1466-8238.2009.00446.x.

Beguería, S., Spanu, V., Navas, A., Machín, J., Angulo-Martínez, M., 2013. Modeling the spatial distribution of soil properties by generalized least squares regression: Toward a general theory of spatial variates. J. Soil Water Conserv. 68, 172–184. https://doi.org/10.2489/jswc.68.3.172.

Bianchini, G., Natali, C., Di Giuseppe, D., Beccaluva, L., 2012. Heavy metals in soils and sedimentary deposits of the Padanian Plain (Ferrara, Northern Italy): characterisation and biomonitoring. J. Soils Sediment. 12, 1145–1153. https://doi.org/10.1007/s11368-012-0538-5.

Bird, P., Comber, S.D.W., Gardner, M.J., Ravenscroft, J.E., 1996. Zinc inputs to coastal waters from sacrificial anodes. Sci. Total. Environ. 181, 257–264. https://doi.org/10.1016/0048-9697(95)05025-6.

Bonifacio, E., Falsone, G., Piazza, S., 2010. Linking Ni and Cr concentrations to soil mineralogy: does it help to assess metal contamination when the natural background is high? J. Soils Sediment. 10, 1475–1486. https://doi.org/10.1007/s11368-010-0244-0.

Crossland, C.J., Baird, D., Ducrotoy, J.-P., Lindeboom, H., Buddemeier, R.W., Dennison, W.C., et al., 2005. The Coastal Zone — a Domain of Global Interactions. In: Crossland, C.J., Kremer, H.H., Lindeboom, H.J., Marshall Crossland, J.I., Le Tissier, M.D.A. (Eds.), Coast. Fluxes Anthr. Land-Ocean Interact. Coast. Zone Proj. Int. Geosph.-Biosphere Programme. Springer, Berlin, Heidelberg, pp. 1–37. https://doi.org/10.1007/3-540-27851-6_1.

Dev, R., Praved, P.H., Nallusamy, B., Nazeer, M.N., Sreeraj, P., Srinivas, R., et al., 2026. Monsoon-driven seasonal dynamics of trace metal contamination and ecological risk in sediments of multiple ecosystems, Mandapam group of islands, Gulf of Mannar, India. Gondwana Res. 158, 277–293. https://doi.org/10.1016/j.gr.2026.06.004.

Dung, T.T.T., Cappuyns, V., Swennen, R., Phung, N.K., 2013. From geochemical background determination to pollution assessment of heavy metals in sediments and soils. Rev. Environ. Sci. Biotechnol. 12, 335–353. https://doi.org/10.1007/s11157-013-9315-1.

Edwards, B.D., 2002. Variations in sediment texture on the northern Monterey Bay National Marine Sanctuary continental shelf. Mar. Geol. 181, 83–100. https://doi.org/10.1016/S0025-3227(01)00262-6.

U.S. EPA. Methods for Collection, Storage and Manipulation of Sediments for Chemicaland Toxicological Analyses: Technical Manual. Washington, DC, USA: 2001.

Gao, X., Yang, Y., Wang, C., 2012. Geochemistry of organic carbon and nitrogen in surface sediments of coastal Bohai Bay inferred from their ratios and stable isotopic signatures. Mar. Pollut. Bull. 64, 1148–1155. https://doi.org/10.1016/j.marpolbul.2012.03.028.

Gazzi, P., Zuffa, G.G., 1970. Le Arenarie Paleogeniche dell'Appeninno Emiliano. Mineral. Petrogr. Acta 16, 97–137.

Gazzi, P., Zuffa, G.G., Gandolfi, G., Paganelli, L., 1973. Provenienza e Dispersione Litoranea delle Sabbie delle Spiagge Adriatiche fra le Foci dell'Isonzo e del Foglia: Inquadramento Regionale. Mem. Della Soc. Geol. Ital. 12, 1–37.

Greggio, N., Giambastiani, B.M.S., Campo, B., Dinelli, E., Amorosi, A., 2017. Sediment composition, provenance, and Holocene paleoenvironmental evolution of the Southern Po River coastal plain (Italy). Geol. J. 53, 914–928. https://doi.org/10.1002/gj.2934.

Hakanson, L., 1980. An ecological risk index for aquatic pollution control.a sedimentological approach. Water Res. 14, 975–1001. https://doi.org/10.1016/0043-1354(80)90143-8.

Hickson, C.J., Juras, J., 1986. Sample contamination by grinding. Can. Miner. 24, 585–589.

Horowitz, A.J., 1991. A primer on sediment-trace element chemistry, second ed. U.S. Geological Survey, Denver, CO, USA.

Jose, J., Krishnakumar, A., Adhipa, V.R., Krishnan, K.A., 2026. Integrated assessment of the environmental stress and human health risks associated with potentially toxic elements in Ashtamudi estuarine sediments, India. Environ. Geochem. Health 48, 456. https://doi.org/10.1007/s10653-026-03310-9.

Koukina, S.E., Lobus, N.V., Peresypkin, V.I., Dara, O.M., Smurov, A.V., 2017. Abundance, distribution and bioavailability of major and trace elements in surface sediments from the Cai River estuary and Nha Trang Bay (South China Sea, Vietnam). Estuar. Coast. Shelf Sci. 198, 450–460. https://doi.org/10.1016/j.ecss.2016.03.005.

Lachance, G.R., Traill, R.J., 1966. Practical Solution to the Matrix Problem in X-Ray Analysis. Can. Spectrosc. 11, 43–48.

Loring, D.H., Rantala, R.T.T., 1992. Manual for the geochemical analyses of marine sediments and suspended particulate matter. Earth Sci. Rev. 32, 235–283. https://doi.org/10.1016/0012-8252(92)90001-A.

Maicu, F., Alessandri, J., Pinardi, N., Verri, G., Umgiesser, G., Lovo, S., et al., 2021. Downscaling With an Unstructured Coastal-Ocean Model to the Goro Lagoon and the Po River Delta Branches. Front. Mar. Sci. 8, 647781. https://doi.org/10.3389/fmars.2021.647781.

Majlesi, S., Akkanen, J., Roivainen, P., Tuovinen, T.S., Sorvari, J., Naarala, J., et al., 2021. Transfer of elements relevant to radioactive waste into chironomids and fish in boreal freshwater bodies. Sci. Total Environ. 791, 148218. https://doi.org/10.1016/j.scitotenv.2021.148218.

Marinov, D., Zaldívar, J.M., Norro, A., Giordani, G., Viaroli, P., 2008. Integrated modelling in coastal lagoons: Sacca di Goro case study. Hydrobiologia 611, 147–165. https://doi.org/10.1007/s10750-008-9451-8.

Matys Grygar, T., Popelka, J., 2016. Revisiting geochemical methods of distinguishing natural concentrations and pollution by risk elements in fluvial sediments. J. Geochem. Explor. 170, 39–57. https://doi.org/10.1016/j.gexplo.2016.08.003.

Migani, F., Borghesi, F., Dinelli, E., 2015. Geochemical characterization of surface sediments from the northern Adriatic wetlands around the Po river delta. Part I: Bulk composition and relation to local background. J. Geochem. Explor. 156, 72–88. https://doi.org/10.1016/j.gexplo.2015.05.003.

Monte, C. do N., Paula de Castro Rodrigues, A., Galvão de Campos, B., Moreira, L.B., Grebbe, B., de Figueiredo Eufrasio Pauly, G., et al., 2025. Influence of seasonality on

the toxicity and metals bioavailability after the resuspension of sediments from a tropical estuary. Estuar. Coast Shelf Sci. 315, 109167. https://doi.org/10.1016/j.ecss.2025.109167.

Müller, J., 1969. Index of geoaccumulation in sediments of the Rhine River. Geol. J. 2, 108–118.

Newton, A., Icely, J., Cristina, S., Brito, A., Cardoso, A.C., Colijn, F., et al., 2014. An overview of ecological status, vulnerability and future perspectives of European large shallow, semi-enclosed coastal systems, lagoons and transitional waters. Estuar. Coast Shelf Sci. 140, 95–122. https://doi.org/10.1016/j.ecss.2013.05.023.

Picone, S., Alvisi, F., Dinelli, E., Morigi, C., Negri, A., Ravaioli, M., et al., 2008. New insights on late Quaternary palaeogeographic setting in the Northern Adriatic Sea (Italy). J. Quat. Sci. 23, 489–501. https://doi.org/10.1002/jqs.1152.

Province of Ferrara, 2007. Caratterizzazione granulometrica, geochimica e microbiologica dei sedimenti della Sacca di Goro. Water Resources and Environmental Protection Service, U.O.P.C. – Coastal Waters and Fisheries Management Unit, Ferrara.

Rahhou, A., Layachi, M., Akodad, M., El Ouamari, N., Aknaf, A., Skalli, A., et al., 2022. Assessment of the trophic status of Marchica Lagoon (Ne Morocco, Mediterranean) after restoration activities using trophic index (trix): seasonal and spatial variations. Appl. Ecol. Environ. Res. 20, 4667–4679. https://doi.org/10.15666/aeer/2006_46674679.

Rousseau, C., Baraud, F., Leleyter, L., Gil, O., 2009. Cathodic protection by zinc sacrificial anodes: Impact on marine sediment metallic contamination. J. Hazard. Mater. 167, 953–958. https://doi.org/10.1016/j.jhazmat.2009.01.083.

Rusydi, A.F., 2018. Correlation between conductivity and total dissolved solid in various type of water: A review. IOP Conf. Ser. Earth Environ. Sci. 118, 012019. https://doi.org/10.1088/1755-1315/118/1/012019.

Saccani, E., Delavari, M., Dolati, A., Pandolfi, L., Barbero, E., Tassinari, R., et al., 2022. Geochemistry of basaltic blueschists from the Deyader Metamorphic Complex (Makran Accretionary Prism, SE Iran): new constraints for magma generation in the Makran sector of the Neo-Tethys. J. Asian Earth Sci. 228, 105141. https://doi.org/10.1016/j.jseaes.2022.105141.

Sammartino, I., 2004. Heavy-metal anomalies and bioavailability from soils of southeastern Po plain. GeoActa 3, 35–42.

Shepard, F.P., 1954. Nomenclature based on sand-silt-clay ratios. J. Sediment. Res. 24, 151–158. https://doi.org/10.1306/D4269774-2B26-11D7-8648000102C1865D.

Simeoni, U., Fontolan, G., Tessari, U., Corbau, C., 2007. Domains of spit evolution in the Goro area, Po Delta, Italy. Geomorphology 86, 332–348. https://doi.org/10.1016/j.geomorph.2006.09.006.

Srivastava, D., Dubey, C.P., Banerji, U.S., Joshi, K.B., 2024. Geochemical trends in sedimentary environments using PCA approach. J. Earth Syst. Sci. 133, 122. https://doi.org/10.1007/s12040-024-02306-2.

Summa, D., Turolla, E., Lanzoni, M., Tamisari, E., Castaldelli, G., Tamburini, E., 2023. Life cycle assessment (lCA) of two different oyster (Crassostrea gigas) farming strategies in the Sacca di Goro, Northern Adriatic Sea, Italy. Resources 12. https://doi.org/10.3390/resources12060062.

Tamburini, E., Turolla, E., Lanzoni, M., Moore, D., Castaldelli, G., 2022. Manila clam and Mediterranean mussel aquaculture is sustainable and a net carbon sink. Sci. Total Environ. 848, 157508. https://doi.org/10.1016/j.scitotenv.2022.157508.

The European Parliament, 2008. The council of the European Union. Directive 2008/56/ec of the European parliament and of the council of 17 June 2008 establishing a framework for community action in the field of marine environmental policy (Marine Strategy Framework Directive). European Union, Brussels, Belgium.

Thompson, G., Bankston, D.C., 1970. Sample contamination from grinding and sieving determined by emission spectrometry. Appl. Spectrosc. 24, 210–219. https://doi.org/10.1366/000370270774371886.

Tomlinson, D.L., Wilson, J.G., Harris, C.R., Jeffrey, D.W., 1980. Problems in the assessment of heavy-metal levels in estuaries and the formation of a pollution index. Helgol. Meeresunters 33, 566–575. https://doi.org/10.1007/BF02414780.

Van, H.-T., Hoang, V.H., Nga, L.T.Q., Nguyen, V.Q., 2024. Effects of Zn pollution on soil: pollution sources, impacts and solutions. Results Surf. Interfaces 17, 100360. https://doi.org/10.1016/j.rsurfi.2024.100360.

Viaroli, P., Marinov, D., Bodini, A., Giordani, G., Galbiati, L., Somma, F., et al., 2007. Analysis of clam farming scenarios in the Sacca di Goro Lagoon. Transit. Waters Monogr. 1, 71–92. https://doi.org/10.1285/i18252273v1n1p71.

Zaldívar, J.M., Cattaneo, E., Plus, M., Murray, C.N., Giordani, G., Viaroli, P., 2003. Long-term simulation of main biogeochemical events in a coastal lagoon: Sacca Di Goro (Northern Adriatic Coast, Italy). Cont. Shelf Res. 23, 1847–1875. https://doi.org/10.1016/j.csr.2003.01.001.

Zonta, R., Cassin, D., Pini, R., Dominik, J., 2019. Assessment of heavy metal and As contamination in the surface sediments of Po delta lagoons (Italy). Estuar. Coast. Shelf Sci. 225, 106235. https://doi.org/10.1016/j.ecss.2019.05.017.